

## Optical Frequency Synthesis and Comparison with Uncertainty at the $10^{-19}$ Level

Long-Sheng Ma,<sup>1,2\*†</sup> Zhiyi Bi,<sup>2\*</sup> Albrecht Bartels,<sup>3\*</sup>  
 Lennart Robertsson,<sup>1</sup> Massimo Zucco,<sup>1</sup> Robert S. Windeler,<sup>4</sup>  
 Guido Wilpers,<sup>3</sup> Chris Oates,<sup>3</sup> Leo Hollberg,<sup>3</sup>  
 Scott A. Diddams<sup>3\*†</sup>

A femtosecond laser-based optical frequency synthesizer is referenced to an optical standard, and we use it to demonstrate the generation and control of the frequency of electromagnetic fields over 100 terahertz of bandwidth with fractional uncertainties approaching 1 part in  $10^{19}$ . The reproducibility of this performance is verified by comparison of different types of femtosecond laser-based frequency synthesizers from three laboratories.

At present, microwave frequency standards based on the ground-state hyperfine transition in cesium atoms have fractional frequency uncertainties at the level of 1 part in  $10^{15}$  (1). However, new optical frequency standards (1) and clocks (2, 3) using ultrastable lasers (4, 5) locked to optical transitions in laser-cooled ions and atoms have the potential to be orders of magnitude more stable and accurate. For example, the stability of neutral calcium and mercury ion optical frequency standards already exceeds that of the best microwave standards by one or two orders of magnitude (2), and the fractional frequency uncertainty of optical standards based on single ions is anticipated to approach  $10^{-18}$  (6). However, such an extremely stable and accurate standard is of little value if its frequency cannot be readily distributed to users and compared to those of other standards based on various atomic species operating at different frequencies.

One of the most compelling motivations for the development of advanced atomic frequency standards is that their intercomparison would allow one to search for possible time variations of fundamental constants (7, 8). For example, laboratory-based tests of the stability of the fine-structure constant  $\alpha$  show no time dependence at the present measurement limit of  $\sim 10^{-15}$  per year (9, 10), whereas astronomical

measurements indicate that  $\alpha$  could have been smaller than its present value by a factor of  $10^{-5}$  in the early universe some 10 billion years ago (11). The next generation of optical frequency standards should enable searches at the level of  $10^{-18}$  per year. However, these searches require a low-noise, broadband ( $>100$  THz) frequency synthesizer that is able to phase-coherently generate an arbitrary optical (or microwave) frequency at its output given an optical frequency reference input. Within this context, we demonstrate that an optical frequency synthesizer using a mode-locked femtosecond laser can operate in such a

manner with a fractional frequency uncertainty approaching 1 part in  $10^{19}$ .

The use of a mode-locked laser for optical frequency metrology was first demonstrated with picosecond lasers (12, 13), with the comb of frequencies emitted from the laser serving as an “optical frequency ruler” or “synthesizer.” The spacing of the comb teeth is given by the repetition rate  $f_{\text{rep}}$  at which pulses are emitted; the overall frequency offset of the comb teeth is given by  $f_{\text{ceo}}$ . Recent experiments (14–19) have demonstrated that the frequency comb associated with a femtosecond mode-locked laser can be readily controlled and is more versatile and precise than existing technologies (20).

We search for potential limitations in the femtosecond laser synthesizer approach by rigorously comparing four such synthesizers that use two different types of construction (20). The basic scheme of our measurements is to compare pairs of femtosecond laser synthesizers (labeled by indices 1 and 2) and verify with optical heterodyne techniques that the output modes have their expected frequency positions relative to a continuous-wave reference laser with frequency  $f_L = 456$  THz (Fig. 1). The mode spacing (i.e., repetition rate) of the two synthesizers can be written as

$$f_{\text{rep}1} = (f_L - f_{\text{ceo}1} - f_{b1})/N_1 \quad (1)$$

$$f_{\text{rep}2} = (f_L - f_{\text{ceo}2} - f_{b2})/N_2 \quad (2)$$

where  $f_{b1, b2}$  are the beat frequencies between  $f_L$  and modes  $N_{1,2}$  of the respective femtosecond

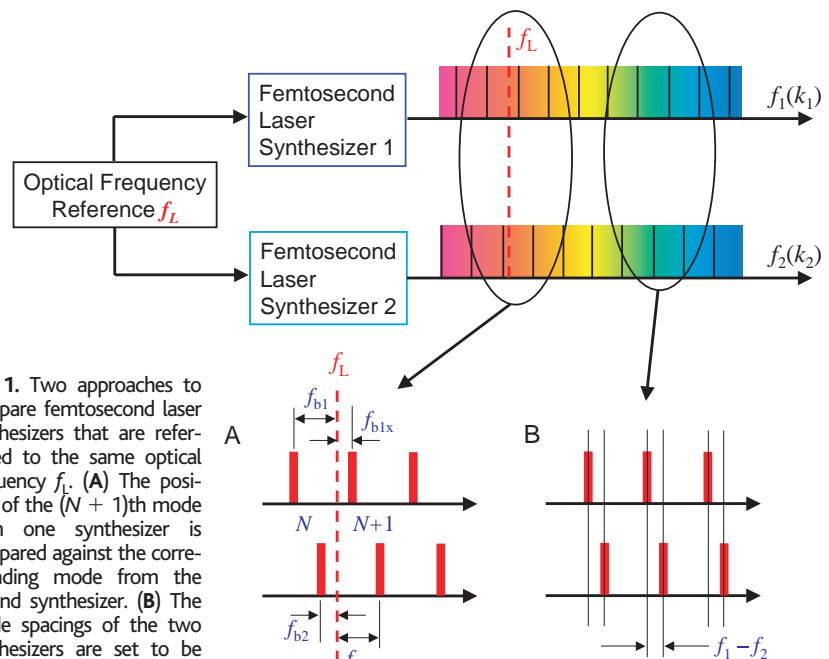


**Fig. 1.** Two approaches to compare femtosecond laser synthesizers that are referenced to the same optical frequency  $f_L$ . **(A)** The position of the  $(N + 1)$ th mode from one synthesizer is compared against the corresponding mode from the second synthesizer. **(B)** The mode spacings of the two synthesizers are set to be equal, thereby enabling the comparison of groups of modes ( $\sim 1000$ ) from each synthesizer in an arbitrary region of the optical spectrum.

<sup>1</sup>Bureau International des Poids et Mesures (BIPM), Pavillon de Breteuil, 92312 Sèvres, France. <sup>2</sup>Physics Department, East China Normal University (ECNU), Shanghai 200062, China. <sup>3</sup>National Institute of Standards and Technology (NIST), 325 Broadway, Boulder, CO 80305, USA. <sup>4</sup>OFS Laboratories, 700 Mountain Avenue, Murray Hill, NJ 07974, USA.

\*These authors contributed equally to this work.  
 †To whom correspondence should be addressed. E-mail: lsma@phy.ecnu.edu.cn (L.S.M.), sdiddams@boulder.nist.gov (S.A.D.)

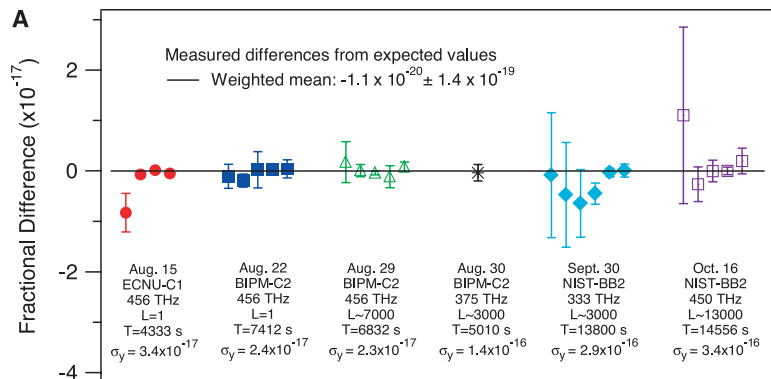


**Fig. 2. (A)** Summary of comparisons of three femtosecond laser synthesizers (BIPM-C2, ECNU-C1, and NIST-BB2) with a fourth synthesizer (NIST-BB1) on six different days in 2003. Also given are the number of comb lines ( $L$ ) used in the comparison, the total averaging time ( $T$ ) in seconds, and the 1-s Allan deviation  $\sigma_y$  for each comparison. **(B)** Relative fractional frequency instability as given by the Allan deviation for (i) our multiline comparison of optical

frequency synthesizers BIPM-C2 and NIST-BB1 at 456 THz, (ii) the optical transfer oscillator of (18) comparing a continuous-wave laser and its second harmonic, and (iii) the high-quality microwave synthesizer of (24). Curves iv and v are the upper limits of instabilities of femtosecond laser-based synthesizers connecting microwave and optical domains as reported in (25) and (16), respectively.

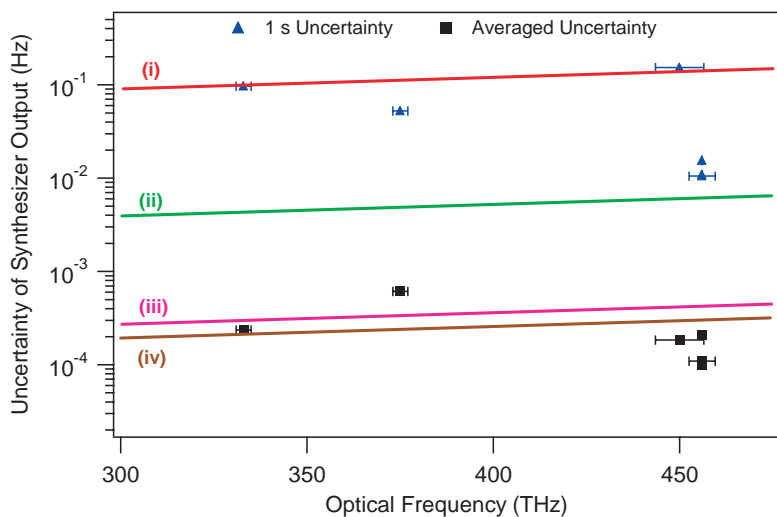
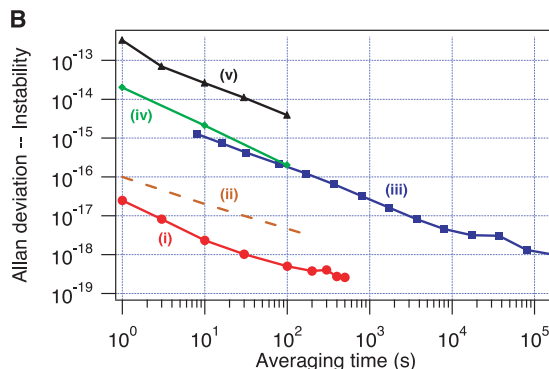


**Fig. 3.** Uncertainty of the optical frequency output of a femtosecond laser frequency synthesizer. Shown are uncertainties at averaging times of 1 s ( $\blacktriangle$ ) and several hours ( $\blacksquare$ ). The frequency error bars on these points indicate the spectral width over which the measurements were made. The various lines indicate the uncertainty limits imposed by (i) the Doppler-induced fluctuations at 1 s, (ii) the 1-s uncertainty introduced by the phase locks controlling the femtosecond synthesizer, (iii) the 1-s fundamental shot noise limitation for the control of the femtosecond synthesizer, and (iv) the estimated limit due to differential Doppler shifts occurring in the control and measurement systems on a 1-hour time scale.

synthesizer. The frequencies of the output modes are then given by

$$f_1(k_1) = f_L - f_{b1} + k_1 \times (f_L - f_{ce01} - f_{b1})/N_1 \quad (3)$$

$$f_2(k_2) = f_L - f_{b2} + k_2 \times (f_L - f_{ce02} - f_{b2})/N_2 \quad (4)$$

where  $k_{1,2} = 0, \pm 1, \pm 2, \dots$ . In our experiments, we require  $N_1 = N_2 = N$ , such that  $\Delta f_{\text{rep}} = f_{\text{rep1}} - f_{\text{rep2}}$  and  $\Delta f = f_1(k_1) - f_2(k_2)$  are independent of the frequency  $f_L$ . Therefore, using Eqs. 1 to 4,  $\Delta f_{\text{rep}}$  and  $\Delta f$  can be determined from  $f_{ce01}$ ,  $f_{ce02}$ ,  $f_{b1}$ ,  $f_{b2}$ ,  $k_1$ ,  $k_2$ , and  $N$ . This enables high-precision tests of the spectral purity and intrinsic noise of the two combs themselves.

In the case of Fig. 1A, with  $f_{\text{rep1}} \sim f_{\text{rep2}}$  but not necessarily equal, we can compare the fre-

quencies of single lines adjacent to mode  $N$  from each of the two combs (i.e.,  $k_1 = k_2 = 1$ ). This method does not require time synchronization between the optical pulse trains from the two synthesizers. When  $f_{ce01}$ ,  $f_{ce02}$ ,  $f_{\text{rep1}}$ , and  $f_{\text{rep2}}$  are controlled as described in Eqs. 1 to 4, the expected difference frequency between the  $k = 1$  lines of two combs can be written as

$$f_1(1) - f_2(1) = (f_{b2} - f_{b1}) + [(f_{ce02} + f_{b2}) - (f_{ce01} + f_{b1})]/N \quad (5)$$

This difference can be determined experimentally by subtracting the two measured beats  $f_{b1x}$  and  $f_{b2x}$ :

$$f_1(1) - f_2(1) = f_{b1x} - f_{b2x} \quad (6)$$

In a second case (Fig. 1B), we require  $f_{\text{rep1}} = f_{\text{rep2}}$ . This allows the use of groups of lines

from each of the two combs with  $k_1 = k_2 = k$  to generate the frequency difference signal. In this case, the expected beat frequency between the two combs can be written as

$$f_1(k) - f_2(k) = f_{ce02} - f_{ce01} \quad (7)$$

When the relative phase between the optical pulse trains from the two synthesizers is set to zero (i.e., the pulses from each synthesizer reach the detector at the same time), all the modes that are appropriately phased generate a strong beat signal with signal-to-noise ratio as high as 60 dB within a 300-kHz bandwidth (21).

Three femtosecond laser synthesizers (BIPM-C2, ECNU-C1, and NIST-BB2) were compared with a fourth synthesizer (NIST-BB1) on 6 days over a period of several months. A summary of these frequency comparisons (Fig. 2A) is plotted as the difference between the measured frequencies and the values predicted by Eqs. 5 to 7. On each day, the heterodyne beat of interest was recorded with a frequency counter for total integration times of several thousand seconds. For each date in Fig. 2A, the data points are the results obtained with different gate times and experimental values of  $f_{ce0}$  and  $f_b$ . The statistical uncertainties shown on the points are used as weights in computing the weighted mean (22). These uncertainties are determined from the calculation of the Allan deviation (23). Such a weighting accounts for the presence of flicker-like noise in the data at longer averaging times and provides a realistic (larger) estimate of the uncertainty. Using standard statistical methods (22), we combined all the data from the 6 days to calculate the weighted mean. The result is equal to  $-1.1 \times 10^{-20}$ , with an uncertainty of  $1.4 \times 10^{-19}$ , corresponding to a 95% confidence level determined from a  $\chi^2$  analysis (22). Both the weighted mean and the uncertainty are normalized by the compared optical frequency to give the fractional values presented. It can thus be concluded that within this confidence level, no systematic effects are detectable at a level of  $1.4 \times 10^{-19}$ .

Figure 2B (curve i) shows an example of the computed Allan deviation for the frequency comparison (method of Fig. 1B) between BIPM-C2 and NIST-BB1 at 456 THz. The very low Allan deviation of  $\sim 2.3 \times 10^{-17}$  at 1 s is achieved when the beams from the two femtosecond lasers are made to be mostly collinear with the 456-THz laser that controls each synthesizer. This implies that the path length fluctuations from the two synthesizers to the heterodyne photodetector are common mode at an approximate level of  $<10$  nm in 1 s of averaging. This low instability enables us to reach statistical uncertainties as low as a few parts in  $10^{19}$  with less than 1000 s of averaging (Fig. 2B). Also shown in Fig. 2B are Allan deviations from other optical and microwave frequency synthesizers.

Figure 3 shows the short-term (1 s) and averaged uncertainties obtained from our measurements, along with measured and projected uncertainties associated with the laser control systems, Doppler shifts, and fundamental shot noise. The short-term (1 s) uncertainty arises from differential mechanical vibrations and variations in air pressure and temperature. The estimated level of these fluctuations (Fig. 3, line i) is in agreement with the measurements across the optical spectrum, except near the frequency  $f_L = 456$  THz where we could arrange the optical paths collinearly for maximum common-mode suppression. The limit set by the performance of the laser control (Fig. 3, line ii) is only a factor of 1.5 below the 1-s uncertainty near 456 THz. The estimated shot noise-limited uncertainty at 1-s averaging for the control of the femtosecond laser synthesizer relative to  $f_L$  is shown in Fig. 3, line iii.

Instabilities on longer time scales or frequency offsets that result in systematic errors are of greater concern. In our comparisons, the various synthesizers were separated by  $\sim 2$  m on a steel table. With temperature variations of  $\sim 0.1^\circ\text{C}$  per hour, the thermal expansion of the steel results in a fractional Doppler shift on the order of a few parts in  $10^{18}$ . We have attempted to cancel this effect by arranging the optical paths for our experiments in a symmetric fashion with as much common-mode rejection as possible. In addition, the relatively long data acquisition times of several hours provide some immunity by averaging over temperature fluctuations on the 100- to 1000-s time scale. In principle, the control system compensates for all Doppler shifts inside the control loop path at frequency  $f_L = 456$  THz; however, because of dispersion (or physically different paths) this is not the case for the emitted frequencies far from  $f_L$ . For example, if the nonlinear optical fiber in BIPM-C2 and ECNU-C1 expands at the same rate given above, the resulting Doppler shift for the frequencies near 333 THz is  $\sim 200$   $\mu\text{Hz}$ , which corresponds to a fractional shift of  $5 \times 10^{-19}$  (Fig. 3, line iv). This indicates that longer averaging times ( $\geq 100,000$  s) or direct mea-

surement and compensation of all Doppler shifts would be required to reduce the uncertainty below the level of  $10^{-19}$ .

Considering the very different designs of these synthesizers (broadband operation versus nonlinear microstructure fiber), it is notable that our data do not point to the existence of any fundamental limitations to the uncertainty. Our results appear to be limited mainly by noise of a technical nature (thermal and mechanical fluctuations) and total integration time. The reproducibility demonstrated in our experiments firmly establishes the femtosecond laser synthesizer as a reliable tool for optical frequency comparisons with uncertainties approaching  $10^{-19}$ , and demonstrates its value for precision measurements in experimental physics.

#### References and Notes

- P. Gill, Ed., *Proceedings of the 6th Symposium on Frequency Standards and Metrology* (World Scientific, Singapore, 2002).
- S. A. Diddams et al., *Science* **293**, 825 (2001).
- J. Ye, L.-S. Ma, J. Hall, *Phys. Rev. Lett.* **87**, 270801 (2001).
- B. C. Young, F. C. Cruz, W. M. Itano, J. C. Bergquist, *Phys. Rev. Lett.* **82**, 3799 (1999).
- C. W. Oates, E. A. Curtis, L. Hollberg, *Opt. Lett.* **25**, 1603 (2000).
- H. G. Dehmelt, *IEEE Trans. Instrum. Meas.* **31**, 83 (1982).
- S. G. Karshenboim, *Can. J. Phys.* **78**, 639 (2000).
- J. D. Prestage, R. J. Tjoelker, L. Maleki, *Phys. Rev. Lett.* **74**, 3511 (1995).
- H. Marion et al., *Phys. Rev. Lett.* **90**, 150801 (2003).
- S. Bize et al., *Phys. Rev. Lett.* **90**, 150802 (2003).
- J. K. Webb et al., *Phys. Rev. Lett.* **87**, 091301 (2001).
- J. N. Eckstein, A. I. Ferguson, T. W. Hänsch, *Phys. Rev. Lett.* **40**, 847 (1978).

- Th. Udem, R. Holzwarth, T. W. Hänsch, *Nature* **416**, 233 (2002).
- Th. Udem, J. Reichert, R. Holzwarth, T. W. Hänsch, *Phys. Rev. Lett.* **82**, 3568 (1999).
- Th. Udem, J. Reichert, R. Holzwarth, T. W. Hänsch, *Opt. Lett.* **24**, 881 (1999).
- R. Holzwarth et al., *Phys. Rev. Lett.* **85**, 2264 (2000).
- S. A. Diddams et al., *Opt. Lett.* **27**, 58 (2002).
- J. Stenger et al., *Phys. Rev. Lett.* **88**, 073601 (2002).
- M. Zimmermann et al., *Opt. Lett.* **29**, 310 (2004).
- See supporting data on Science Online.
- R. K. Shelton et al., *Science* **293**, 1286 (2001).
- I. Lira, *Evaluating the Measurement Uncertainty* (Institute of Physics, Bristol, UK, 2002).
- D. W. Allan, *IEEE Trans. Ultrason. Ferroelect. Freq. Control* **34**, 647 (1987).
- A. Sen Gupta, D. Popovic, F. L. Walls, in *Proceedings of the 1999 Joint Meeting of the European Frequency and Time Forum (EFTF) and the IEEE International Frequency Control Symposium (FCS)*, Besançon, France, 13 to 16 April 1999 (IEEE, Piscataway, NJ, 1999), pp. 615–619.
- A. Bartels, S. A. Diddams, T. M. Ramond, L. Hollberg, *Opt. Lett.* **28**, 663 (2002).
- We thank T. Ramond, R. Fox, and J. Bergquist for their contributions to this work, and J. Hall, D. Wineland, and J. Ye for their thoughtful comments on this manuscript. The work at NIST was funded in part by NASA. The project at ECNU was funded in part by the Science and Technology Commission of Shanghai Municipality (01DJGK014, 022261033), Shanghai Municipal Education Commission, National Science Foundation of China (10274020), and Ministry of Education, China (02106).

#### Supporting Online Material

www.sciencemag.org/cgi/content/full/303/5665/1843/DC1

Materials and Methods

SOM Text

Fig. S1

References

24 December 2003; accepted 13 February 2004

## A Molecular Elevator

Jovica D. Badjić,<sup>1</sup> Vincenzo Balzani,<sup>2</sup> Alberto Credi,<sup>2\*</sup>  
Serena Silvi,<sup>2</sup> J. Fraser Stoddart<sup>1\*</sup>

We report the incrementally staged design, synthesis, characterization, and operation of a molecular machine that behaves like a nanoscale elevator. The operation of this device, which is made of a platformlike component interlocked with a trifurcated riglike component and is only 3.5 nanometers by 2.5 nanometers in size, relies on the integration of several structural and functional molecular subunits. This molecular elevator is considerably more complex and better organized than previously reported artificial molecular machines. It exhibits a clear-cut on-off reversible behavior, and it could develop forces up to around 200 piconewtons.

Biomotor molecules are extremely complex machines, the detailed structures and precise working mechanisms of which have been elucidated only in a very few cases (1, 2). Chemists are trying to construct much

simpler molecular machines as a logical step toward mimicking the actions of biomotor molecules (3–5). In the past few years, several different kinds (6–14) of artificial molecular machines have been designed and constructed.

Here, we describe the incrementally staged design, bottom-up construction, characterization, and chemically driven operation of a two-component molecular machine that behaves like a nanometer-scale elevator. This nanoactuator, which is circa (ca.) 2.5 nm in height with diameter of ca. 3.5 nm, consists of a trifurcated riglike

<sup>1</sup>California NanoSystems Institute and Department of Chemistry and Biochemistry, University of California, Los Angeles, 405 Hilgard Avenue, Los Angeles, CA 90095, USA. <sup>2</sup>Dipartimento di Chimica "G. Ciamician," Università di Bologna, Via Selmi 2, 40126 Bologna, Italy.

\*To whom correspondence should be addressed. E-mail: alberto.credi@unibo.it (A.C.); stoddart@chem.ucla.edu (J.F.S.)